20th Australasian Fluid Mechanics Conference
Perth, Australia
5-8 December 2016

Toward the Design of a Synthetic Jet Actuator for use on a Circulation Control Aerofoil and Its Bench Top Characterisation

P. Itsariyapinyo and R.N. Sharma

Department of Mechanical Engineering
University of Auckland, Auckland 1142, New Zealand

Abstract

This paper discusses some considerations on the design of a synthetic jet actuator for use on a circulation control aerofoil and reports on the bench top characterisation of this synthetic jet actuator. The considerations on the design are based on the Coandă effect imposed on the rounded trailing edge of a circulation control aerofoil and flow instabilities which are commonly found on an aerofoil. The radius of the Coandă surface and the width of a jet slot, which determine the efficiency of the circulation control aerofoil, are estimated according to the aerofoil chord length. Flow instabilities' frequencies, such as the vortex shedding and shear layer instability, are dependent on the aerofoil chord length and angle of attack. These frequencies are used to select a diaphragm whose operating frequency range is similar to the range of flow instabilities' frequencies. The bench top characterisation of a synthetic jet actuator was carried out by measuring the internal pressure of the actuator cavity and the jet velocity at its slot exit using a pressure transducer and hot-wire anemometer respectively. The effects of the synthetic jet frequency, voltage applied on the diaphragm, and cavity volume on the performance of the synthetic jet actuator are studied and presented.

Introduction

Circulation control technology was first reported in the late 1930s and has emerged as a high-lift device and alternative flight control surface in recent times. Conventionally, a circulation control aerofoil consists of an air plenum, an orifice, and a Coandă surface. A continuous air jet, supplied from an on-board compressor, is ejected from the orifice. This air jet then makes contact with and entrains on the Coandă surface. Owing to the Kutta-Joukowski theorem, the entrainment of the air jet on the Coandă surface alters the stagnation points of a circulation control aerofoil, which in turn improves the circulation around an aerofoil and increases lift coefficient. Extensive studies on the circulation control technology were undertaken by researchers from various disciplines [8] both experimentally and computationally. In attempts to optimise the efficiency of the circulation control operation, Kweder et al. [10] and Lan and Campbell [11] offered a design guideline and suggested that there are several combinations of the radius of the Coandă surface, the width of an orifice, and the chord length of an aerofoil which could potentially improve the efficiency of the circulation control operation. Nevertheless, continuous jet based applications were largely investigated in the past. Unlike a continuous jet, a synthetic jet uses repetitive blowing jet and suction to suppress flow instabilities while optimising the mass flow rate required to achieve the same degree of improvement yielded by a continuous jet.

A synthetic jet actuator normally consists of an orifice, a cavity, and a diaphragm which is fixed to the other end of a cavity. Upon oscillating a diaphragm outward and inward, successive suction and jet blowing are repeatedly and alternatively occurred at an orifice respectively. A glance into how a synthetic jet actuator is constructed reveals that the jet formation is considerably influenced by the geometrical parameters of an actuator. Gallas et al. [4] formulated a lumped element model (LEM) which models the components of a piezoelectrically driven synthetic jet actuator based on their electrical properties. Sharma [13] presented a fluid-dynamics-based analytical model for synthetic jet actuation and suggested that the geometrical parameters of an actuator and the characteristics of a diaphragm can be optimised to improve the performance of an actuator measured by the synthetic jet velocity from the view point of flow control.

Flow instabilities on an aerofoil are inevitable occurrences. Huang and Lin [6] conducted wind tunnel testing and observed vortex roll-up and vortex shedding on a NACA0012 aerofoil at low Reynolds numbers. They reported that the frequencies of the vortex shedding and shear layer instability vary with the chord Reynolds number and the angle of attack. Yarusevych et al. [15] conducted wind tunnel testing on a NACA0018 aerofoil and their results showed good agreement with Huang and Lin in which the frequencies of the vortex shedding and the shear layer instability (vortex roll-up) decreases and increases as the angle of attack increases. Mollo-Christensen [12] investigated the mixing layer instability, which is normally found at the sub-layer of air jet, by measuring pressure fluctuations at the sub-layer of a continuous air jet emerging from a circular orifice using a microphone. He reported that the air jet sporadically turns into a form of air puff at the Strouhal number of 0.3 and this Strouhal number remains unchanged throughout the range of Reynolds numbers of 100 to 100,000 [3]. Several investigations utilised this typical Strouhal number to effectively reduce noise emitted from an aircraft via delaying jet separation.

This paper concerns 2 issues. The first part will discuss some considerations on the design of a synthetic jet actuator for use on a circulation control aerofoil and the second part will report on the bench top characterisation of this synthetic jet actuator.

Design

In this section, the designs of the aerofoil and synthetic jet actuator are discussed. Furthermore, the considerations on the selection of a diaphragm are mentioned.

Aerofoil Section

Unlike the flow separation control aerofoil which has its synthetic jet actuators installed at the thicker section of an aerofoil, the circulation control aerofoil requires synthetic jet actuators to be installed close to the trailing edge to enable the circulation control operation while minimising the length of the actuator orifice which, otherwise, may retard the synthetic jet velocity and attenuate the synthetic jet frequency. Due to this requirement, the aerofoil section must be thick enough to allow for some spaces at the trailing edge area. Nevertheless, choosing the aerofoil section which is too thick will result in higher drag. Therefore, synthetic jet actuators used in this study are designed for a NACA0015 aerofoil used in another study [7].

Aerofoil Sizing

It is noteworthy that the frequencies of flow instabilities are dependent on the chord Reynolds number. Therefore, sizing the aerofoil chord length in such a manner that the frequencies of flow instabilities would fall close to the actuator diaphragm or cavity Helmholtz resonance frequency will most likely result in having higher synthetic jet velocity actuated at these frequencies which could possibly lead to a more efficient circulation control operation. Since the scope of the study is on a small UAV, the aerofoil chord length is 170 mm.

Coandă surface

The design parameters of the Coandă surface consist of the radius of a curved surface and the width of a jet orifice. It has been concluded by Chang et al. [2] that a continuous jet with higher velocity can push the stagnation points on a circulation control aerofoil further downstream which further improves lift enhancement. The physics behind this occurrence is that the air jet with higher velocity has higher kinetic energy which keeps it attached on the Coandă surface for a longer distance. Instead of using high-velocity jet to achieve higher lift coefficient, fine-tuning the radius of a Coandă surface and the width of a jet orifice can improve the adherability of the air jet on a Coandă surface [10]-[11].

Orifice

The dimensions of an orifice determine the Helmholtz resonance frequency of an actuator (f_H) and the efficiency of the circulation control operation as related to the radius of a Coandă surface.

$$f_H = \sqrt{k_H/m_H} = \frac{c}{2\pi}\sqrt{\frac{A_o}{V_o L_e}} \tag{1}$$

$$L_e = L_o + C_I\sqrt{A_o} \tag{2}$$

As expressed in equation 1 where m_H is the mass of the air jet at an orifice and c is the sound speed, the orifice area (A_o) and the effective length (L_e) of an orifice play important roles in determining the Helmholtz resonance frequency. The effective length of an orifice is expressed in equation 2 where L_o is the actual length of an orifice and C_I is the inertia coefficient [13].

Cavity Volume (V_o)

$$f_D = \sqrt{k_D/m_D} = \frac{1}{2\pi}\sqrt{\frac{\gamma A_D^2 P_0}{V_o m_D}} \tag{3}$$

$$\varsigma = \varsigma_D + \varsigma_H = c_D/2\sqrt{m_D k_D} + c_H/2\sqrt{m_H k_H} \tag{4}$$

As seen in equation 3 where m_D is the mass of a diaphragm, the cavity volume takes part in estimating the diaphragm resonance frequency under the influence of its cavity enclosure (f_D), pneumatic stiffness (k_H), and structural stiffness (k_D). In terms of designing or sizing the cavity volume, an analytical model offered by Sharma [13] showed that the damping ratio of an actuator (ς), as expressed in equation 4 where ς_D is the structural damping ratio, ς_H is the pneumatic damping ratio, c_D is the structural damping coefficient and c_H is the pneumatic damping coefficient, could be reduced by decreasing the cavity volume to achieve higher jet velocity. Guy et al. [5] suggested that the combination of these geometrical parameters can be optimised to maximise the output of a synthetic jet.

Diaphragm

While a piezoelectric diaphragm is more appealing to the aerospace application due its lightweight design, the resonance frequency of this diaphragm is typically higher than those of a loudspeaker. Since the frequencies of flow instabilities found on the current circulation control aerofoil [7] are relatively low. A loudspeaker, which offers low operating range of frequency, is used instead.

Experimental Setup

The bench top characterisation of the synthetic jet actuator consists of 2 parts which are the velocity-based (output jet velocity) and pressure-based (cavity pressure) measurements. The loudspeakers used in this actuator are driven by a signal generator and power amplifier. Therefore, the input parameters are the synthetic jet frequency and applied voltage. The spectral analysis of fluctuating cavity pressures shows that the highest power spectrum peak, which is the diaphragm resonance frequency, is located at 330-390 Hz. Thus, the synthetic jet frequencies of 75-400 Hz are used in the test. Based on the maximum allowable power of the loudspeaker, the applied voltages of 0.5-2.5 V are used. In order to study the effect of the cavity volume, 4 different cavities heights (h) of 0.5, 1.0, 1.5, and 2.0 mm are considered. The cavity diameter of 34 mm, the orifice width of 0.2 mm, the orifice slot length of 32 mm, and the orifice actual length measured from the centre of the cavity of 2 mm are fixed for all cavities.

Velocity-based Experiments

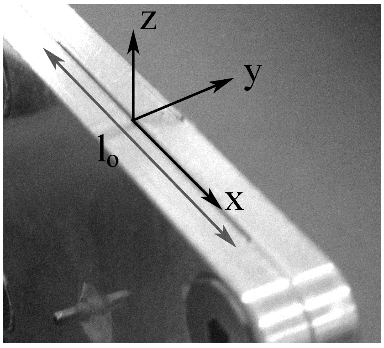

Figure 1. Coordinates of a synthetic jet slot

A hot-wire probe was setup on a traverse unit to measure the synthetic jet velocity with respect to the Cartesian coordinates outlined in Figure 1. The transient time-history velocities, which consist of 32768 samples, are sampled at 24 kHz.

Pressure-based Experiment

4 pressure taps installed at the centres of 4 cavities are used to measure cavity pressures. The transient time-history pressures, which consist of 32768 samples, are sampled at 24 kHz. Like the velocity-based experiment, the cavity pressures are measured for every combination of input parameters.

In order to understand the frequency responses of 4 cavities, the spectral analysis of fluctuating cavity pressures was conducted in a separate experiment where filtered white noise signal is input to the loudspeakers. This white noise signal is cut-off at 4.5 kHz using a low-pass filter. 163840 samples of fluctuating cavity pressures are sampled at 10 kHz. These samples are divided into 10 blocks of 16384 samples to perform FFT and block averaging.

Results and Discussion

The spectral analysis of fluctuating cavity pressures reveals the operating frequency range of a synthetic jet actuator. While velocity-based results directly report on the performance of a synthetic jet actuator, pressure-based results provide some further insights into the behaviour of a synthetic jet actuator. Peak jet velocities obtained from ranges of input parameters are reported in this section. Additionally, peak cavity pressures are also reported to unveil the relationship between the cavity pressure and synthetic jet velocity.

Spectral Analysis of Fluctuating Cavity Pressures

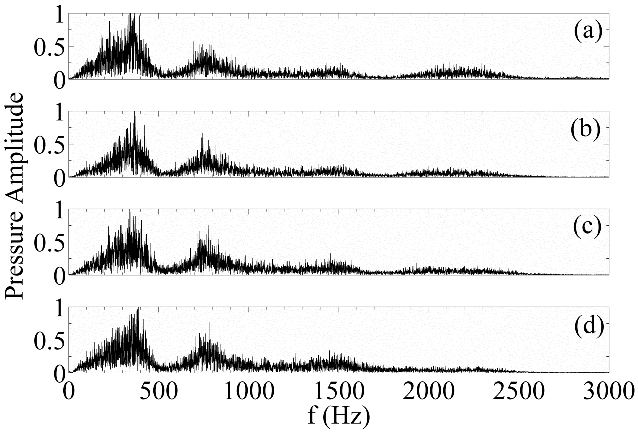

Figure 2. Normalised amplitudes of power spectrum densities of fluctuating cavity pressures obtained from cavity (a) 1 (h = 0.5 mm), (b) 2 (h = 1.0 mm), (c) 3 (h = 1.5 mm), and (d) 4 (h = 2.0 mm).

As reported by the manufacturer [9], the free-air diaphragm resonance frequency of the loudspeaker is estimated to be 570±20% Hz. Upon mounting the loudspeaker to the cavity, whose geometry resembles a bass-reflex enclosure, to form the actuator, the spectral analysis of fluctuating cavity pressures, as seen in Figure 2, reveals that the diaphragm resonance frequency is now split up into 2 peaks at approximately 330-390 Hz and 720-760 Hz. The split-up in diaphragm resonance frequency is common in acoustics when a loudspeaker is mounted to a bass-reflex enclosure [1].

Apart from the diaphragm resonance frequency, a series of white noise signal provided to the loudspeaker is low-pass filtered at 4.5 kHz so that the Helmholtz resonance frequency could be found within this range. According to the frequency responses shown in Figure 2, the third peak of the power spectrum density, which is the Helmholtz resonance frequency, is found at 1.45-1.55 kHz for all the cavities. A very weak power spectrum density found at around 2.0-2.5 kHz is the second peak of the diaphragm resonance frequency.

Although the volume of the fourth cavity is 4 times higher than the first cavity, the diaphragm and Helmholtz resonance frequencies of these 2 cavities are still the same. Theoretically, if the cavity volume increases by a factor of 4, the resonance frequencies should be halved. Therefore, it is important to note that the Helmholtz and diaphragm resonance frequencies' formulas, expressed in equations 1 and 3, are unable to accurately predict the values of these resonance frequencies. The cause of the inaccuracy could be due to the flat shape of the actuator which is considered to be very different from the round shape of a conventional Helmholtz resonator.

Effects of the Cavity Volume (V_o), Synthetic Jet Frequency (f), and Applied Voltage (V) on the Peak Cavity Pressure (P_p) and Peak Jet Velocity (U_p)

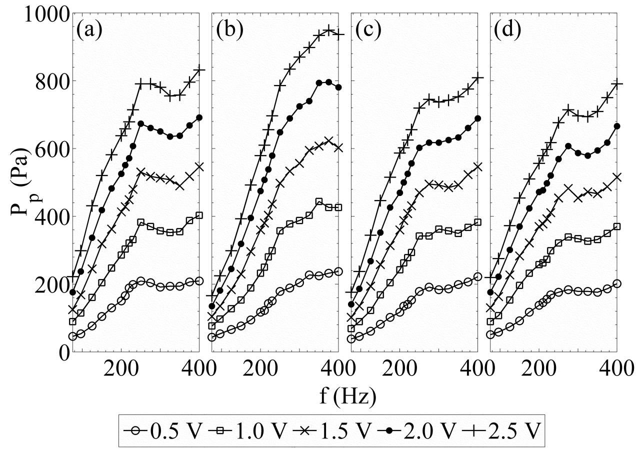

Figure 3. Effects of the cavity volume (represented by cavity height h), synthetic jet frequency, and applied voltage on the peak cavity pressure obtained from cavity (a) 1 (h = 0.5 mm), (b) 2 (h = 1.0 mm), (c) 3 (h = 1.5 mm), and (d) 4 (h = 2.0 mm).

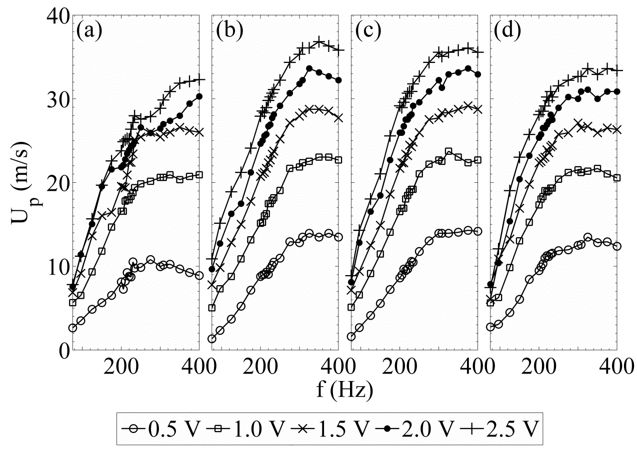

Figure 4. Effects of the cavity volume (represented by cavity height h), synthetic jet frequency, and applied voltage on the peak jet velocity measured at x = 0, y = 0, and z = 1 mm obtained from cavity (a) 1 (h = 0.5 mm), (b) 2 (h = 1.0 mm), (c) 3 (h = 1.5 mm), and (d) 4 (h = 2.0 mm).

Since the cavity volume, synthetic jet frequency, and applied voltage affect both the cavity pressure and jet velocity in a similar manner, their effects on the cavity pressure and jet velocity are discussed in the same section. Figure 3 shows the peak cavity pressures measured from 4 cavities. Figure 4 shows the peak jet velocities measured at x = 0, y = 0, and z = 1 mm of 4 cavities.

The results shown in Figures 3 and 4 reveal that the peak cavity pressure and peak jet velocity exhibit a strong correlation in which the peak cavity pressure could be implicitly used to predict the corresponding peak jet velocity and vice versa. Although the relationship between the displacement of a diaphragm and the cavity pressure has not been investigated in this study, it was reported by Yao et al. [14] that the cavity pressure is linearly proportional to the diaphragm displacement of a synthetic jet actuator. Hence, it is fair to say that the peak cavity pressure would increase if the diaphragm displacement increases.

As seen in Figures 3 and 4, increases in peak cavity pressure and jet velocity can be observed from every cavity volume as the synthetic jet frequency increases and approaches the diaphragm resonance frequency. Positive offsets in peak cavity pressure and jet velocity trends can be acquired when the applied voltage is increased. To a certain extent, the effects of the synthetic jet frequency and applied voltage are predetermined by the manufacturer. For instance, the free-air diaphragm resonance frequency is determined by the structural stiffness of a diaphragm and that the stiffness is dependent on how a diaphragm is constrained to its rim and coil. Since a synthetic jet actuator normally operates at a fixed frequency at a time, increasing an applied voltage would increase the electrical current on a voice coil and the electrodynamic force acting on a diaphragm. Consequently, increasing the applied voltage will most likely result in higher diaphragm displacement, cavity pressure, and jet velocity.

Unlike the effects of the synthetic jet frequency and applied voltage which are somewhat predetermined by the manufacturer, changing the cavity volume can directly affect the stiffness and damping ratio of an actuator structurally and pneumatically. Prior to the discussion, it should be noted that the smallest cavity volume (h = 0.5 mm) is the exceptional case and will be discussed in the last paragraph of this section. At a low frequency range (75-200 Hz), the effect of the cavity volume is not clear as the growth rates of the peak cavity pressure and peak jet velocity trends yielded from all cavities are similar. At a higher frequency range (200-400Hz), the effect of the cavity volume on the peak cavity pressure and peak jet velocity have become apparent. Unlike the second cavity (Figure 3b) which is capable of developing the maximum peak cavity pressure at the diaphragm resonance frequency, declines in peak cavity pressure trends which are obtained from larger cavity volumes (Figures 3c and 3d) are found at the diaphragm resonance frequency where the highest peak cavity pressure is expected.

Similar to the cavity pressure, declines in peak jet velocity trends at a higher frequency range can be clearly observed as the cavity height increases from 1.0 mm to 1.5 mm and 2.0 mm. Due to the increases in damping ratios, the peak jet velocity trends yielded from cavities 3 and 4 are unable to develop the maximum peak at a higher frequency range. Thus, relatively flat trends, illustrated in Figures 4c and 4d, are produced instead.

Theoretically, the first cavity, which has the smallest volume, should have the lowest damping ratio. Therefore, the first cavity should be able to yield the highest peak cavity pressure and jet velocity. However, the results shown in Figures 3a and 4a do not follow the statement. Like the other cavities, the first cavity is capable of generating decent jet velocities over a low frequency range. As the synthetic jet frequency approaches and reaches the diaphragm resonance frequency, sharp drops in peak cavity pressure, as observed in Figure 3a, are evident for every applied voltage case. Similar to the peak cavity pressure, peak jet velocity trends obtained from 1.5-2.5V cases (Figure 4a) struggle to produce the maximum peak. If one looks at this inferior cavity pressure in term of the diaphragm displacement, it is fair to say that the diaphragm movement could be physically restrained or obstructed. After revisiting the datasheet of the loudspeaker, the manufacturer suggested that the cavity height should be at least 0.8 mm to allow for diaphragm deflection. Since the height of the first cavity is 0.5 mm, it is suspected that the diaphragm might have hit the wall as soon as the diaphragm resonance frequency and higher applied voltages are approached and reached.

Conclusions

This paper proposes the ideas of improving the efficiency of a circulation control aerofoil by fine-tuning the geometrical parameters and replacing a continuous jet with a synthetic jet. The spectral analysis of fluctuating cavity pressures reveals that the diaphragm and Helmholtz resonance frequencies' formulas are unable to accurately predict the resonance frequencies of the actuator. It has been found in the study that actuating a synthetic jet near or at the diaphragm resonance frequency results in higher jet velocity which would ultimately lead to an effective flow control if the diaphragm resonance frequency is aligned with the flow instabilities' frequencies on an aerofoil. For a miniature synthetic jet actuator, such as the one used in this study, altering the cavity volume can drastically change the synthetic jet velocity as the cavity volume plays the role in defining both the structural and pneumatic damping ratios of an actuator.

References

[1] Beranek, L.L., Acoustics, Acoustics, American Institute of Physics for the Acoustical Society of America, 1986, 239-258.

[2] Chang, P.A., Slomski, J., Marino, T., Ebert, M.P. & Abramson, J., Full Reynolds-Stress Modeling of Circulation Control Airfoils, in *Applications of Circulation Control Technologies*, editors R.D. Joslin and G.S. Jones, AIAA, 2006, 445-465.

[3] Crow, S.C. & Champagne, F.H., Orderly Structure in Jet Turbulence, Boeing Scientific Research Laboratories. Document D1-82-0991, 1970.

[4] Gallas, Q., Holman, R., Nishida, T., Carrol, B., Sheplak, M. & Cattafesta, L., Lumped Element Modeling of Piezoelectric-Driven Synthetic Jet Actuators, AIAA Journal, **41**, 2, 2003, 240-247.

[5] Guy, Y., McLaughlin, T. & Albertson, J., Effect of Geometric Parameters on the Velocity Output of a Synthetic Jet Actuator, in *40th AIAA Aerospace Sciences Meeting & Exhibit*. AIAA Paper 2002-0126, 2002.

[6] Huang, R.F. & Lin, C.L., Vortex Shedding and Shear-Layer Instability of Wing at Low-Reynolds Numbers, AIAA Journal, **33**, 8, 1995, 1398-1403.

[7] Itsariyapinyo, P. & Sharma, R.N., NACA0015 Circulation Control Airfoil Using Synthetic Jets at Low Angles of Attack and Low Reynolds Number, in *8th AIAA Flow Control Conference.* AIAA Paper 2016-3772, 2016.

[8] Joslin, R.D. & Jones, G.S. (editors) *Applications of Circulation Control Technologies,* Reston, VA, AIAA, 2006.

[9] Kingstate Electronics Corp., Micro Dynamic Speaker KDMG36008-10B, 2008.

[10] Kweder, J., Panther, C.C. & Smith, J.E., Applications of circulation control, yesterday and today, Int. J. Eng., **4**, 5, 2011, 411-429.

[11] Lan, C.E. & Campbell, J.F., Theoretical Aerodynamics of Upper-Surface Blowing Jet-Wing Interaction, NASA, Washington, D.C., 1975.

[12] Mollo-Christensen, E., Jet Noise and Shear Flow Instability Seen From an Experimenter's Viewpoint, Journal of Applied Mechanics, **34**, 1, 1967, 1-7.

[13] Sharma, R.N., Fluid-Dynamics-Based Analytical Model for Synthetic Jet Actuation, AIAA Journal, **45**, 8, 2007, 1841-1847.

[14] Yao, C., Chen, F. & Neuhart, D., Synthetic Jet Flow Field Database for CFD Validation, in *2nd AIAA Flow Control Conference.* AIAA Paper 2004-2218, 2004.

[15] Yarusevych, S., Sullivan, P.E. & Kawall, J.G., On vortex shedding from an airfoil in low-Reynolds-number flows, J. Fluid Mech., **632**, 2009, 245-271.